Kinetics of irreversible adsorption with a particle conformational change: A density expansion approach

Paul R. Van Tassel,[1,2] Julian Talbot,[3] Gilles Tarjus,[1] and Pascal Viot[1]
[1]*Laboratoire Physique Théorique des Liquides, Université Pierre et Marie Curie, 4 place Jussieu, 75252 Paris Cedex 05, France*
[2]*Centre Européen de Calcul Atomique et Moléculaire, Ecole Normale Supérieure de Lyon, Aile LR5, 46, Allée d'Italie, 69364 Lyon Cedex 07, France*
[3]*School of Chemical Engineering, Purdue University, West Lafayette, Indiana 47907*
(Received 11 July 1995)

The kinetics of the irreversible adsorption of particles that undergo a surface induced conformational change may be modeled as a random sequential adsorption of spreading disks. We analyze this process by expanding the governing kinetic equations in a power series of the particle density. In the limit where particles spread instantaneously upon adsorption, the coefficients in the density expansion depend only upon the particle spreading magnitude Σ. In the general case of a finite spreading rate, a renormalization is performed to improve the efficiency of the expansion and the coefficients become functions of Σ and a new variable $\zeta=\rho K_s$, where ρ is the density and K_s is the relative rate of particle spreading. While they are most accurate at low to moderate densities, these expressions may be linked to the known asymptotic kinetics via interpolation formulas to give an approximate solution over the entire density regime, in good agreement with simulation and experiment.

PACS number(s): 68.45.Da, 05.20.−y, 05.70.Ln

I. INTRODUCTION

The adsorption of macromolecules such as proteins [1–7] and colloids [8,9] is often irreversible, that is, desorption and surface diffusion are slow compared to the rate of adsorption. In these cases, the random sequential adsorption (RSA) model [10–13] may apply. In RSA, particles are represented as rigid objects that deposit sequentially at random positions onto a surface. If overlap with a previously placed particle occurs, the attempt is rejected and a new trial position is chosen. This process continues until no additional particles may be placed on the surface. This simple model has been shown to describe many features of the adsorption of colloids [8] and proteins [5–7].

An additional aspect of irreversible adsorption observed experimentally, yet not accounted for in simple RSA models, is the possibility of a particle conformational change following adsorption. Recently, we have studied a RSA model that accounts for a surface induced particle conformational change in the form of a change in particle size following adsorption (i.e., spreading) [14,15]. In one dimension, this model is exactly solvable in the case where the spreading is instantaneous [14]. In two dimensions, computer simulation is required [15]. The purpose of this work is to (i) analyze the kinetics of the two-dimensional case via a series expansion in powers of the density and (ii) to combine this expansion with the known asymptotic behavior towards saturation so as to have an approximate description valid over the entire coverage range. Such a method has already been applied to simple RSA [10,16–18] and to more complicated deposition processes [19–21]. The simple formulas that result may be used to investigate the main kinetic features for a wide range of physical parameters, thus facilitating comparison with experimental results [5].

The kinetic model of spreading disks presented here is a modification of the standard random sequential adsorption model. In the former, disks of diameter σ_α (hereafter referred to as α particles) are deposited randomly and sequentially onto a surface at a rate $k_a c$ per unit area (the c explicitly represents the particle concentration in the bulk phase). Only incoming α particles that do not overlap any preadsorbed particles are allowed to remain on the surface. Once adsorbed, an α particle will spread discretely and symmetrically to a larger diameter σ_β at a rate k_s, provided that the expansion does not cause overlap with any other particles. If the expansion would result in overlap, the original particle remains forever an α particle. If the expansion is successful, the particle is now said to have changed state to become a β particle. In either case, the particle position on the surface remains fixed for the entire run. We have recently reported extensive numerical simulations of this model [15]; throughout this work, results of the density expansion approach will be compared to these "exact" results.

We note that when k_s is zero, one recovers the standard RSA model whose short time kinetics density expansion has appeared elsewhere [10,11,16]. In Sec. II of this work we will discuss the special case where k_s is infinite. In Sec. III we will treat the general case when k_s is finite and nonzero. A formalism for interpolating between the low- and high-density regimes will be given in Sec. IV and a comparison with experimental results in Sec. V.

II. INSTANTANEOUS SPREADING

When the spreading is instantaneous, the governing equations for the kinetics of adsorption of α and β parti-

cles may be obtained by considering the changes introduced by the flux of incoming particles during an infinitesimal interval of time dt. The density of α particles ρ_α increases due to particles landing at positions that satisfy two criteria: (i) there is no overlap with preadsorbed particles and (ii) there is not enough additional space for particle spreading. Similarly, the density of β particles ρ_β increases due to particles that land in positions with space enough to spread. The governing equations may be written as

$$\frac{\partial \rho_\alpha}{\partial t} = k_a c(\Phi_\alpha(\rho,\Sigma) - \Phi_\beta(\rho,\Sigma)) , \tag{1}$$

$$\frac{\partial \rho_\beta}{\partial t} = k_a c \Phi_\beta(\rho,\Sigma) , \tag{2}$$

where ρ_λ is the number density of λ particles (where $\lambda=\alpha$ or β), $\rho=\rho_\alpha+\rho_\beta$ is the total number density, and $k_a c$ is the rate of adsorption per unit area. Φ_λ is the available surface function [11,16] for a λ particle that represents the fractional surface available for adsorption of a λ particle. More specifically, it is equal to the probability that a point chosen at random on the surface will be at least a distance $(\sigma_\lambda+\sigma_\gamma)/2$ from the center of each γ particle, where γ and $\lambda=\alpha$ or β. This function will in general depend upon the total density ρ and the ratio of particles sizes Σ $(=\sigma_\beta/\sigma_\alpha)$. Note that in all irreversible adsorption processes, the total density of adsorbed particles ρ is a monotonically increasing function of time, so one can consider either ρ or t as the relevant variable to describe the evolution of the system.

It is convenient to recast Eqs. (1) and (2) in dimensionless form

$$\frac{\partial \rho_\alpha^*}{\partial t^*} = \Phi_\alpha(\rho^*,\Sigma) - \Phi_\beta(\rho^*,\Sigma) , \tag{3}$$

$$\frac{\partial \rho_\beta^*}{\partial t^*} = \Phi_\beta(\rho^*,\Sigma) , \tag{4}$$

where $\rho_\lambda^* = (\pi\sigma_\alpha^2/4)\rho_\lambda$ and $t^* = k_a c(\pi\sigma_\alpha^2/4)t$. Hereafter, we will drop the asterisks, but all quantities will remain dimensionless.

The available surface function may be written as a sum of contributions involving the various particle density distributions in a manner similar to that introduced in Ref. [11] for the RSA of disks:

$$\Phi_\lambda(\rho,\Sigma) = \sum_{s_\alpha,s_\beta=0}^{\infty} \frac{1}{s_\alpha! s_\beta!} \int d2\cdots d(s_\alpha+s_\beta+1) f_{12}^{\lambda\alpha}\cdots f_{1(s_\alpha+1)}^{\lambda\alpha} f_{1(s_\alpha+2)}^{\lambda\beta}\cdots f_{1(s_\alpha+s_\beta+1)}^{\lambda\beta}$$
$$\times \rho_{\alpha\alpha\cdots\beta\beta\cdots}^{(s_\alpha+s_\beta)}(2,\ldots,s_\alpha+1,s_\alpha+2,\ldots,s_\alpha+s_\beta+1;\rho,\Sigma) . \tag{5}$$

In Eq. (5), the particle positions $\mathbf{r}_i$ have been replaced by i and use has been made of the Mayer functions, which for hard disks take the form $f_{ij}^{\lambda\gamma}=-1$ if $r_{ij}<\sigma_{\lambda\gamma}$ and $f_{ij}^{\lambda\gamma}=0$ if $r_{ij}\geq\sigma_{\lambda\gamma}$. $\rho_{\alpha\alpha\cdots\beta\beta\cdots}^{(s_\alpha+s_\beta)}(2,\ldots,s_\alpha+1,s_\alpha+2,\ldots,s_\alpha+s_\beta+1;\rho,\Sigma)$ denotes the density function associated with finding s_α particles of species α centered at $2,\ldots,s_\alpha+1$ and s_β particles of species β centered at $s_\alpha+2,\ldots,s_\alpha+s_\beta+1$. The first term ($s_\alpha=s_\beta=0$) is taken to be unity. Each successive term accounts for the blockage of a newly placed particle (at position 1) by s_α α particles and s_β β particles simultaneously. The form of the Mayer functions ensures that the blocking particles are within the required proximity to position 1. The sign of the product of Mayer functions may be understood by the following example. When $s_\alpha+s_\beta=1$, the product of Mayer functions will be negative and the integral accounts for the decrease in fractional area accessible to adsorption due to blockage by the presence of single particles. When $s_\alpha+s_\beta=2$, the product is positive and corrects for the overcounting associated with regions on the surface blocked by pairs. In general, the term associated with blockage by $n+1$ particles accounts for the overcounting of the term associated with the blockage by n particles. Note that because of the finite number of neighboring particles that can be placed around a given particle, the sum in Eq. (5) has a finite number of nonzero terms.

The goal is to expand Eq. (5) up to third order in density. Clearly, only terms where $s_\alpha+s_\beta\leq 3$ will be required. We begin by expanding the available surface function and the partial, many-body densities in terms of the total one-body density $(\rho=\rho_\alpha+\rho_\beta)$ as

$$\Phi_\lambda(\rho,\Sigma) = 1 + \sum_{n=1}^{3} a_{\lambda n}(\Sigma)\rho^n + O(\rho^4) , \tag{6}$$

$$\rho_{\alpha\alpha\cdots\beta\beta\cdots}^{(s_\alpha+s_\beta)}(1,\ldots,s_\alpha+s_\beta,\rho,\Sigma) = \sum_{n=1}^{3} A_n^{\alpha\alpha\cdots\beta\beta\cdots}(1,\ldots,n;\Sigma)\rho^n + O(\rho^4) . \tag{7}$$

It is clear that $A_n^{\alpha\alpha\cdots\beta\beta\cdots}=0$ for $n<s_\alpha+s_\beta$. Since both Φ_α and Φ_β equal $1+O(\rho)$, Eqs. (3) and (4) imply that $\rho_\beta=\rho+O(\rho^2)$ and $\rho_\alpha=O(\rho^2)$. This can be understood physically by considering that the adsorption of α particles is a "two-body" process in that it requires at least one preadsorbed particle to prevent its spreading. We thus have $A_1^\alpha=0$, $A_1^\beta=1$, and $A_n^\alpha=-A_n^\beta$ for $n>1$. To obtain the particle densities up to second order in ρ, we differentiate ρ_α in Eq. (7) with respect to time and equate it to Eq. (3):

$$\frac{\partial \rho_\alpha}{\partial t}=2A_2^\alpha\rho+O(\rho^2)=\int d2(f_{12}^{\alpha\beta}-f_{12}^{\beta\beta})\rho+O(\rho^2)\ , \tag{8}$$

$$A_2^\alpha=-A_2^\beta=\tfrac{1}{2}\int d2(f_{12}^{\alpha\beta}-f_{12}^{\beta\beta})\ , \tag{9}$$

where we now drop the explicit Σ dependence of the coefficients.

To obtain the pair densities to lowest (second) order, we consider the following kinetic equation for the evolution of the β-β pair density, which generalizes the Kirkwood-Salsburg hierarchy derived for standard RSA [11]:

$$\frac{\partial}{\partial t}(\rho_{\beta\beta}^{(2)}(1,2))=(\Phi_{\beta\beta}(1,2^o)+\Phi_{\beta\beta}(2,1^o))$$
$$=2\Phi_{\beta\beta}(1,2^o)\ , \tag{10}$$

where $\Phi_{\beta\beta}$ is a mixed one-particle, one-cavity density function whose expression is a special case of the formula

$$\Phi_{\lambda\mu}(1,2^o)=(1+f_{12}^{\lambda\mu})\sum_{s_\alpha,s_\beta=0}^{\infty}\frac{1}{s_\alpha!s_\beta!}\int d3\cdots d(s_\alpha+s_\beta+2)f_{23}^{\mu\alpha}\cdots f_{2(s_\alpha+2)}^{\mu\alpha}f_{2(s_\alpha+3)}^{\mu\beta}\cdots f_{2(s_\alpha+s_\beta+2)}^{\mu\beta}$$
$$\times\rho_{\lambda\alpha\alpha\cdots\beta\beta\cdots}^{(1+s_\alpha+s_\beta)}(1,3,\ldots,s_\alpha+2,\ldots,s_\alpha+s_\beta+2;\rho,\Sigma)\ , \tag{11}$$

where $\lambda=\alpha,\beta$ and $\mu=\alpha,\beta$. Equations (10) and (11) can be interpreted as follows. To create a new pair of β particles at positions 1 and 2, one must have both a preexisting β particle centered on 1 and a cavity centered on 2 available for the insertion of a β particle or, equivalently, a cavity centered on 1 and a preexisting β particle centered on 2. $\Phi_{\lambda\mu}(1,2^o)$ is then the probability density associated with simultaneously finding a λ particle at 1 and a cavity large enough to house a μ particle at 2 (the superscript o indicates a cavity). The second equality of Eq. (10) results from the symmetry of these functions with respect to the choice of position for a given species. Expanding both sides of Eq. (10) to first order in density and employing the definitions in Eqs. (7) and (11), we obtain

$$A_2^{\beta\beta}(1,2)=1+f_{12}^{\beta\beta}\ . \tag{12}$$

Similar equations exist for the time evolution of the other pair densities

$$\frac{\partial}{\partial t}(\rho_{\alpha\beta}^{(2)}(1,2))=(\Phi_{\alpha\beta}(1,2^o)+\Phi_{\beta\alpha}(2,1^o)-\Phi_{\beta\beta}(2,1^o))\ , \tag{13}$$

$$\frac{\partial}{\partial t}(\rho_{\alpha\alpha}^{(2)}(1,2))=2(\Phi_{\alpha\alpha}(1,2^o)-\Phi_{\alpha\beta}(1,2^o))\ , \tag{14}$$

whose solutions to first order yield the coefficients

$$A_2^{\alpha\beta}(1,2)=\tfrac{1}{2}(f_{12}^{\alpha\beta}-f_{12}^{\beta\beta})\ , \tag{15}$$

$$A_2^{\alpha\alpha}(1,2)=0\ . \tag{16}$$

Equation (16) illustrates that the existence of a pair of α particles requires the presence of at least three particles; indeed, to prevent both α particles from spreading, a preadsorbed third particle must have been present.

We now have enough information to obtain the third-order coefficients of the various pair densities by expanding Eqs. (10), (13), and (14) up to second order in ρ and employing the definitions in Eqs. (7) and (11). This yields the coefficients

$$A_3^{\beta\beta}(1,2)=\tfrac{1}{3}(1+f_{12}^{\beta\beta})\left[\int d3\,f_{23}^{\alpha\beta}(f_{13}^{\alpha\beta}-f_{13}^{\beta\beta})-6A_2^\alpha+2\int d3\,f_{23}^{\beta\beta}f_{13}^{\beta\beta}\right]\ , \tag{17}$$

$$A_3^{\alpha\beta}(1,2)=\tfrac{1}{3}(1+f_{12}^{\alpha\beta})\left[\tfrac{1}{2}\int d3\,f_{23}^{\beta\beta}(f_{13}^{\alpha\beta}-f_{13}^{\beta\beta})+\tfrac{1}{2}\int d3\,f_{13}^{\alpha\alpha}(f_{23}^{\alpha\beta}-f_{23}^{\beta\beta})+\int d3\,f_{13}^{\alpha\beta}f_{23}^{\beta\beta}\right]$$
$$-\tfrac{1}{3}(1+f_{12}^{\beta\beta})\left[\tfrac{1}{2}\int d3\,f_{13}^{\alpha\beta}(f_{23}^{\alpha\beta}-f_{23}^{\beta\beta})+\int d3\,f_{13}^{\beta\beta}f_{23}^{\beta\beta}-3A_2^\alpha\right]\ , \tag{18}$$

$$A_3^{\alpha\alpha}(1,2)=\tfrac{2}{3}(f_{12}^{\alpha\alpha}-f_{12}^{\alpha\beta})A_2^\alpha+\tfrac{1}{3}(1+f_{12}^{\alpha\alpha})\int d3\,f_{23}^{\alpha\beta}(f_{13}^{\alpha\beta}-f_{13}^{\beta\beta})-\tfrac{1}{3}(1+f_{12}^{\alpha\beta})\int d3\,f_{23}^{\beta\beta}(f_{13}^{\alpha\beta}-f_{13}^{\beta\beta})\ . \tag{19}$$

We now expand Eq. (8) to second order to obtain

$$\frac{\partial \rho_\alpha}{\partial t} = 2A_2^\alpha \rho + (2A_2^\alpha a_{\alpha 1} + 3A_3^\alpha)\rho^2 + O(\rho^3) . \quad (20)$$

Matching the second-order terms from Eqs. (5) and (20), we find

$$A_3^\alpha = \tfrac{1}{3} A_2^\alpha \int d2(f_{12}^{\alpha\alpha} - 4f_{12}^{\alpha\beta} + f_{12}^{\beta\beta}) + \tfrac{1}{6}\int d2\,d3(f_{12}^{\alpha\beta} f_{13}^{\alpha\beta} - f_{12}^{\beta\beta} f_{13}^{\beta\beta})(1 + f_{23}^{\beta\beta}) + \tfrac{1}{6}\int d2\,d3(f_{12}^{\alpha\alpha} f_{13}^{\alpha\beta} - f_{12}^{\alpha\beta} f_{13}^{\beta\beta})(f_{23}^{\alpha\beta} - f_{23}^{\beta\beta}) . \quad (21)$$

All that remains is to find the triplet densities to lowest (third) order. The governing kinetic equations read

$$\frac{\partial}{\partial t}\rho_{\beta\beta\beta}^{(3)}(1,2,3) = 3\Phi_{\beta\beta\beta}(1,2,3^o) , \quad (22)$$

$$\frac{\partial}{\partial t}\rho_{\alpha\beta\beta}^{(3)}(1,2,3) = 2\Phi_{\alpha\beta\beta}(1,2,3^o) + \Phi_{\beta\beta\alpha}(2,3,1^o) - \Phi_{\beta\beta\beta}(2,3,1^o) , \quad (23)$$

$$\frac{\partial}{\partial t}\rho_{\alpha\alpha\beta}^{(3)}(1,2,3) = \Phi_{\alpha\alpha\beta}(1,2,3^o) + 2\Phi_{\alpha\beta\alpha}(1,3,2^o) - 2\Phi_{\alpha\beta\beta}(1,3,2^o) , \quad (24)$$

$$\frac{\partial}{\partial t}\rho_{\alpha\alpha\alpha}^{(3)}(1,2,3) = 3\Phi_{\alpha\alpha\alpha}(1,2,3^o) - 3\Phi_{\alpha\alpha\beta}(1,2,3^o) . \quad (25)$$

In the above expressions, $\Phi_{\lambda\mu\nu}(1,2,3^o)$, where λ, μ, and ν denote α or β, represents the probability density associated with having a λ particle at position 1 and a μ particle at position 2 and a cavity large enough to accommodate a ν particle at position 3. These functions can be expressed in a similar manner as the pair terms in Eq. (11). Expanding both sides of Eqs. (22)–(25) to second order using the definitions of Eqs. (7) and (11) and the coefficients of Eqs. (12), (15), and (16), we obtain the coefficients

$$A_3^{\beta\beta\beta}(1,2,3) = (1+f_{12}^{\beta\beta})(1+f_{13}^{\beta\beta})(1+f_{23}^{\beta\beta}) , \quad (26)$$

$$A_3^{\alpha\beta\beta}(1,2,3) = -(1+f_{12}^{\alpha\beta})(1+f_{13}^{\alpha\beta})(1+f_{23}^{\beta\beta}) \times [\tfrac{1}{2}(f_{12}^{\beta\beta} + f_{13}^{\beta\beta}) + \tfrac{1}{3} f_{12}^{\beta\beta} f_{13}^{\beta\beta}] , \quad (27)$$

$$A_3^{\alpha\alpha\beta}(1,2,3) = \tfrac{1}{6}(1+f_{12}^{\alpha\alpha})(1+f_{13}^{\alpha\beta})(1+f_{23}^{\alpha\beta}) \times [2f_{13}^{\beta\beta} f_{23}^{\beta\beta} + f_{12}^{\alpha\beta}(f_{23}^{\beta\beta} + f_{13}^{\beta\beta}) + 2f_{13}^{\beta\beta} f_{23}^{\beta\beta} f_{12}^{\beta\beta}] , \quad (28)$$

$$A_3^{\alpha\alpha\alpha}(1,2,3) = 0 . \quad (29)$$

The last of these equations implies that the presence of triplets of α particles will require at least a four-body interaction.

We now have all the coefficients needed to expand Φ_α and Φ_β to third order in density. Substituting the known expansions of the densities in Eq. (8) into Eq. (5), we obtain the desired coefficients. These appear in the Appendix.

Figure 1 displays the density expansion of the partial and total densities to second and third order versus time for $\Sigma = 1.1$ and 1.5. The kinetics is rather well described with the third-order density expansion at short times. For longer times, the total density may approach an asymptotic value (as when $\Sigma = 1.1$) or may diverge (as when $\Sigma = 1.5$). We note that, in general, the range of validity decreases with increasing Σ. Additionally, for $\Sigma = 1.5$, the second-order expansion has a greater range of accuracy than the third-order expansion, indicating a fortuitous cancellation between three- and higher-body effects even at intermediate coverages.

III. FINITE SPREADING RATE

When the spreading rate is finite, the (dimensionless) kinetic equations take the form

$$\frac{\partial \rho_\alpha}{\partial t} = \Phi_\alpha(\rho, \Sigma, K_s) - K_s \rho_\alpha \Psi_{\alpha\beta}(\rho, \Sigma, K_s) , \quad (30)$$

$$\frac{\partial \rho_\beta}{\partial t} = K_s \rho_\alpha \Psi_{\alpha\beta}(\rho, \Sigma, K_s) , \quad (31)$$

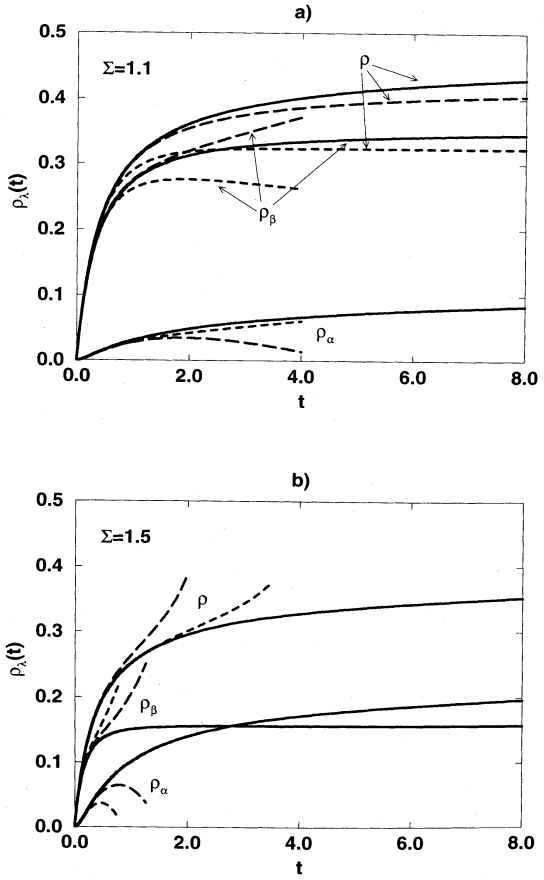

FIG. 1. Second- (short dashed line) and third- (dashed line) order density expansion of the reduced total and partial densities as function of reduced time for instantaneous spreading ($K_s \to +\infty$) with (a) $\Sigma = 1.1$ and (b) $\Sigma = 1.5$. Also shown are simulation results (solid line).

where $\Psi_{\alpha\beta}$ is the probability for a given α particle on the surface to have space available to spread, that is, to be at least a distance $(\sigma_\alpha+\sigma_\beta)/2$ from all other α particles and at least a distance σ_β from all β particles; it will in general be a function of Σ and K_s, where K_s is defined as

$$K_s=\frac{k_s}{k_a c\frac{\pi\sigma_\alpha^2}{4}} . \tag{32}$$

This general case differs from the case of instantaneous spreading [$K_s\to+\infty$ in Eqs. (1) and (2)] in that Φ_β has been replaced in Eqs. (30) and (31) by $K_s\rho_\alpha\Psi_{\alpha\beta}$. This term accounts for the fact that all α particles on the surface (not only the last ones inserted) may spread during the infinitesimal interval of time between t and $t+dt$. We seek a density expansion of both Φ_α and the product $\rho_\alpha\Psi_{\alpha\beta}$. The former is defined as in Eqs. (5) and (6), the latter by

$$\rho_\alpha\Psi_{\alpha\beta}(\rho,\Sigma,K_s)=\sum_{s_\alpha,s_\beta=0}^{\infty}\frac{1}{s_\alpha!s_\beta!}\int d2\cdots d(s_\alpha+s_\beta+1)f_{12}^{\beta\alpha}\cdots f_{1(s_\alpha+1)}^{\beta\alpha}f_{1(s_\alpha+2)}^{\beta\beta}\cdots f_{1(s_\alpha+s_\beta+1)}^{\beta\beta}$$
$$\times\rho_{\alpha\alpha\cdots\beta\beta\cdots}^{(s_\alpha+s_\beta+1)}(1,\ldots,s_\alpha+1,s_\alpha+2,\ldots,s_\alpha+s_\beta+1;\rho,\Sigma,K_s) . \tag{33}$$

The one-body, two-body, etc., densities can be expanded in powers of the total density as in Eq. (8), but now the coefficients $A_n^{\alpha\alpha\cdots\beta\beta\cdots}$ are functions of both Σ and K_s.

One must recover the instantaneous spreading case in the limit when $K_s\to\infty$. Because at short times, terms such as $\rho_\alpha K_s$ remain finite even as $K_s\to\infty$, we choose to renormalize the kinetic equations by changing variables from (ρ,K_s) to (ρ,ζ), where $\zeta=\rho K_s$. This change of variables reexpresses the kinetic equation as

$$\left[\frac{\partial\rho_\alpha}{\partial t}\right]_\zeta+\left[\frac{\partial\rho_\alpha}{\partial\zeta}\right]_\rho\left[\frac{\zeta}{\rho}\right]\left[\frac{\partial\rho}{\partial t}\right]_{K_s}$$
$$=\Phi_\alpha(\rho,\zeta)-\left[\frac{\zeta}{\rho}\right]\rho_\alpha\Psi_{\alpha\beta}(\rho,\zeta) , \tag{34}$$

where

$$\left[\frac{\partial\rho_\alpha}{\partial t}\right]_\zeta=\Phi_\alpha\sum_{n=1}^{\infty}nA_n^\alpha(\zeta)\rho^{n-1}$$
$$=A_1^\alpha(\zeta)+[A_1^\alpha(\zeta)a_{\alpha1}(\zeta)+2A_2^\alpha(\zeta)]\rho+\cdots , \tag{35}$$

$$\left[\frac{\partial\rho_\alpha}{\partial\zeta}\right]_\rho=\sum_{n=1}^{\infty}\frac{\partial A_n^\alpha}{\partial\zeta}\rho^n , \tag{36}$$

$$\left[\frac{\partial\rho}{\partial t}\right]_{K_s}=\Phi_\alpha=1+\sum_{n=1}^{\infty}a_{an}(\zeta)\rho^n , \tag{37}$$

$$\rho_\alpha\Psi_{\alpha\beta}=\rho_\alpha+\sum_{n=2}^{\infty}b_n(\zeta)\rho^n , \tag{38}$$

where the explicit dependence of the coefficients on the new variable ζ (but not that on Σ) is noted. To zeroth order in density, Eq. (34) gives

$$A_1^\alpha(\zeta)+\zeta\frac{\partial A_1^\alpha}{\partial\zeta}=1-\zeta A_1^\alpha(\zeta) , \tag{39}$$

whose solution is $A_1^\alpha(\zeta)=(1-e^{-\zeta})/\zeta$. Notice that as $\zeta\to\infty$ (fast spreading), $A_1^\alpha\to0$ and $\rho_\alpha\sim\rho^2$, consistent with the results obtained above for instantaneous spreading.

To first order in density, Eq. (34) gives

$$A_1^\alpha(\zeta)a_{\alpha1}(\zeta)+2A_2^\alpha(\zeta)+\zeta\frac{\partial A_2^\alpha}{\partial\zeta}+\zeta a_{\alpha1}(\zeta)\frac{\partial A_1^\alpha}{\partial\zeta}$$
$$=a_{\alpha1}(\zeta)-\zeta A_2^\alpha(\zeta)-\zeta b_2(\zeta) . \tag{40}$$

To solve Eq. (40), we need values for $a_{\alpha1}(\zeta)$ and $b_2(\zeta)$. The former may be obtained from a first-order expansion of Φ_α using the known value of $A_1^\alpha(\zeta)$, which leads to

$$a_{\alpha1}(\zeta)=\int d2\,f_{12}^{\alpha\beta}+A_1^\alpha(\zeta)\int d2(f_{12}^{\alpha\alpha}-f_{12}^{\alpha\beta}) . \tag{41}$$

The latter can be obtained from the density expansion of Eq. (38), but this requires knowledge of the leading coefficients to the pair densities.

Generalizing the results obtained for the instantaneous spreading case, the kinetic equation for the three needed pair densities may be written as

$$\frac{\partial}{\partial t}\rho_{\alpha\alpha}^{(2)}(1,2)=2\Phi_{\alpha\alpha}(1,2^\circ)-2K_s\rho_{\alpha\alpha}^{(2)}(1,2)\Psi_{\alpha\alpha\beta}(1,2^\circ) , \tag{42}$$

$$\frac{\partial}{\partial t}\rho_{\alpha\beta}^{(2)}(1,2)=\Phi_{\beta\alpha}(2,1^\circ)+K_s\rho_{\alpha\alpha}^{(2)}(1,2)\Psi_{\alpha\alpha\beta}(1,2^\circ)$$
$$-K_s\rho_{\alpha\beta}^{(2)}(1,2)\Psi_{\beta\alpha\beta}(2,1^\circ) , \tag{43}$$

$$\frac{\partial}{\partial t}\rho_{\beta\beta}^{(2)}(1,2)=2K_s\rho_{\alpha\beta}^{(2)}(1,2)\Psi_{\beta\alpha\beta}(2,1^\circ) , \tag{44}$$

where $\Phi_{\lambda\mu}(1,2^\circ)$ is defined as in Eq. (11) and

$$\rho^{(2)}_{\lambda\alpha}(1,2)\Psi_{\lambda\alpha\beta}(1,2^o)=(1+f^{\lambda\beta}_{12})\sum_{s_\alpha,s_\beta=0}^{\infty}\frac{1}{s_\alpha!s_\beta!}\int d3\cdots d(s_\alpha+s_\beta+2)f^{\beta\alpha}_{23}\cdots f^{\beta\alpha}_{2(s_\alpha+2)}$$
$$\times f^{\beta\beta}_{2(s_\alpha+3)}\cdots f^{\beta\beta}_{2(s_\alpha+s_\beta+2)}\rho^{(s_\alpha+s_\beta+2)}_{\lambda\alpha\alpha\cdots\beta\beta\cdots}(1,\ldots,s_\alpha+s_\beta+2;\rho,\Sigma,\zeta) \quad (45)$$

is the probability density associated with finding a particle of type λ at position 1 and an α particle at position 2, which has enough space to spread and become a β particle. Renormalization of Eqs. (42)–(44) by introducing the variable ζ gives

$$\left[\frac{\partial\rho^{(2)}_{\alpha\alpha}(1,2)}{\partial t}\right]_\zeta+\left[\frac{\partial\rho^{(2)}_{\alpha\alpha}(1,2)}{\partial\zeta}\right]_\rho\left[\frac{\zeta}{\rho}\right]\Phi_\alpha$$
$$=2\Phi_{\alpha\alpha}(1,2^o)-2\left[\frac{\zeta}{\rho}\right]\rho^{(2)}_{\alpha\alpha}(1,2)\Psi_{\alpha\alpha\beta}(1,2^o)\,, \quad (46)$$

$$\left[\frac{\partial\rho^{(2)}_{\alpha\beta}(1,2)}{\partial t}\right]_\zeta+\left[\frac{\partial\rho^{(2)}_{\alpha\beta}(1,2)}{\partial\zeta}\right]_\rho\left[\frac{\zeta}{\rho}\right]\Phi_\alpha$$
$$=\Phi_{\beta\alpha}(2,1^o)+\left[\frac{\zeta}{\rho}\right]\rho^{(2)}_{\alpha\alpha}(1,2)\Psi_{\alpha\alpha\beta}(1,2^o)$$
$$-\rho^{(2)}_{\alpha\alpha}(1,2)\Psi_{\beta\alpha\beta}(2,1^o)\,, \quad (47)$$

$$\left[\frac{\partial\rho^{(2)}_{\beta\beta}(1,2)}{\partial t}\right]_\zeta+\left[\frac{\partial\rho^{(2)}_{\beta\beta}(1,2)}{\partial\zeta}\right]_\rho\left[\frac{\zeta}{\rho}\right]\Phi_\alpha$$
$$=2\left[\frac{\zeta}{\rho}\right]\rho^{(2)}_{\alpha\beta}(1,2)\Psi_{\beta\alpha\beta}(2,1^o)\,. \quad (48)$$

When $\zeta\to+\infty$, corresponding to instantaneous spreading, Eqs. (50)–(52) properly reduce to Eqs. (12), (15), and (16).

The coefficient b_2 of the expansion of $\rho_\alpha\Psi_{\alpha\beta}$, Eq. (38), is then

$$b_2(\zeta)=\int d2\,f^{\alpha\beta}_{12}A^{\alpha\alpha}_2(1,2;\zeta)+\int d2\,f^{\beta\beta}_{12}A^{\alpha\beta}_2(1,2;\zeta) \quad (53)$$

and the solution to Eq. (40) is

$$A^\alpha_2(\zeta)=\frac{1}{\zeta^2}\left\{(-\tfrac{1}{2}\zeta^2e^{-\zeta}+\zeta-1+e^{-\zeta})\int d2\,f^{\alpha\beta}_{12}\right.$$
$$+(4e^{-\zeta}-3-e^{-2\zeta}+2\zeta)\int d2(f^{\alpha\alpha}_{12}-f^{\alpha\beta}_{12})$$
$$+(\tfrac{1}{2}\zeta^2-\zeta+\tfrac{1}{2}-e^{-\zeta}+\zeta e^{-\zeta}+\tfrac{1}{2}e^{-2\zeta})$$
$$\left.\times\int d2(f^{\alpha\beta}_{12}-f^{\beta\beta}_{12})\right\}. \quad (54)$$

First, we will consider Eq. (46), which to first order in density yields

$$2A^{\alpha\alpha}_2(1,2;\zeta)+\zeta\frac{\partial A^{\alpha\alpha}_2}{\partial\zeta}=2(1+f^{\alpha\alpha}_{12})A^\alpha_1(\zeta)$$
$$-2\zeta(1+f^{\alpha\beta}_{12})A^{\alpha\alpha}_2(1,2;\zeta)\,. \quad (49)$$

The presence of the Mayer function implies that $A^{\alpha\alpha}_2$ is a piecewise function, which may be written in a compact form as

$$A^{\alpha\alpha}_2(1,2;\zeta)$$
$$=(1+f^{\alpha\alpha}_{12})\frac{2}{\zeta^2}[-f^{\alpha\beta}_{12}(\zeta+e^{-\zeta}-1)$$
$$+(1+f^{\alpha\beta}_{12})(\tfrac{1}{2}+\tfrac{1}{2}e^{-2\zeta}-e^{-\zeta})]\,. \quad (50)$$

Notice that for $r_{12}<\sigma_\alpha$, $A^{\alpha\alpha}_2$ vanishes since no pair of overlapping particles can exist. The single solutions to Eqs. (47) and (48) may be obtained in the same way:

$$A^{\alpha\beta}_2(1,2;\zeta)=(1+f^{\alpha\beta}_{12})\frac{1}{\zeta^2}[-f^{\beta\beta}_{12}(\tfrac{1}{2}\zeta^2-\tfrac{1}{2}+e^{-\zeta}-\tfrac{1}{2}e^{-2\zeta})+(1+f^{\beta\beta}_{12})(\zeta-1+2e^{-\zeta}-\zeta e^{-\zeta}-e^{-2\zeta})]\,, \quad (51)$$

$$A^{\beta\beta}_2(1,2;\zeta)=(1+f^{\beta\beta}_{12})\frac{1}{\zeta^2}(\tfrac{1}{2}\zeta^2-\zeta+\tfrac{1}{2}-e^{-\zeta}+\zeta e^{-\zeta}+\tfrac{1}{2}e^{-2\zeta})\,. \quad (52)$$

We now have enough information to obtain $a_{\alpha 2}(\zeta)$ of the expansion of Φ_α:

$$a_{\alpha 2}(\zeta)=A^\alpha_2(\zeta)\int d2(f^{\alpha\alpha}_{12}-f^{\alpha\beta}_{12})$$
$$+\tfrac{1}{2}\int d2\,d3\,f^{\alpha\alpha}_{12}f^{\alpha\alpha}_{13}A^{\alpha\alpha}_2(2,3;\zeta)$$
$$+\tfrac{1}{2}\int d2\,d3\,f^{\alpha\beta}_{12}f^{\alpha\beta}_{13}A^{\beta\beta}_2(2,3;\zeta)$$
$$+\int d2\,d3\,f^{\alpha\alpha}_{12}f^{\alpha\beta}_{13}A^{\alpha\beta}_2(2,3;\zeta)\,, \quad (55)$$

which gives us the expansion of the kinetics up to second order in density. We point out that all the integrals appearing in the various coefficients up to second order can be determined analytically or can be reduced to a single straightforward integration.

Figure 2 shows the low-density expansion along with the simulation data for moderate ($K_s=1$) and fast ($K_s=10$) spreading rates. Notice that the deviation of

the low-density expansion from the simulation data occurs at a smaller density for larger values of K_s. As observed for the case of an infinite spreading rate, an asymptotic value is reached by the total density while the partial densities diverge. Finally, the range of validity was observed to decrease with increasing Σ.

IV. INTERPOLATION SCHEMES

We now possess a solution for the random sequential adsorption of spreading disks accurate at low density. The high-density, asymptotic regime of the standard RSA of disks has been analyzed using geometrical and probabilistic arguments and it has been shown that the approach to saturation for the RSA with spreading problem is the same as for standard RSA [15], that is, at long times

$$\frac{\partial\rho}{\partial t}\sim t^{-3/2}\sim[\rho_\infty-\rho(t)]^3 , \tag{56}$$

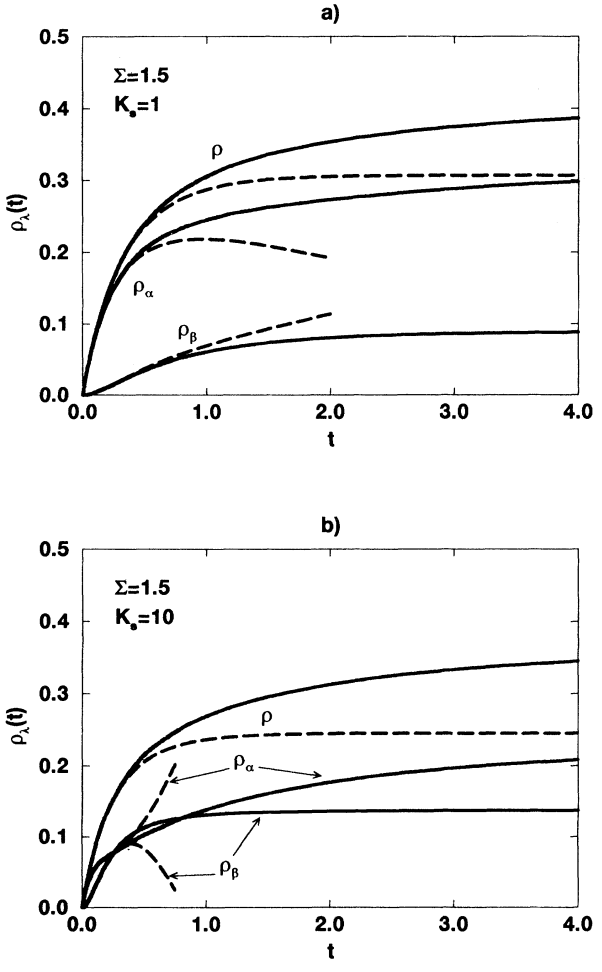

FIG. 2. Second-order density expansion (dashed line) of the reduced total and partial densities as functions of reduced time for $\Sigma=1.5$ and (a) $K_s=1$ and (b) $K_s=10$. Also shown are simulation results (solid line).

where ρ_∞ is the saturation density.

Unlike the low- and high-density limits, the intermediate loading regime cannot be simply analyzed due to both the importance of many-body effects and the lack of a simple structure for the available surface as exists close to saturation. In order to obtain an analytical expression for the entire range of density, we propose here two interpolation formulas that match the density expansion at low to intermediate coverage and the known asymptotic kinetics at high coverage. This procedure was used for standard RSA [16,22], where it was shown to provide an accurate approximation.

A. Direct method

In the case of instantaneous spreading, we now possess the low-density expansion up third order. We may then use the following interpolation formula, first used for standard RSA [22]:

$$\frac{\partial\rho}{\partial t}=\frac{(1-x)^3}{1+b_1x+b_2x^2} , \tag{57}$$

where $x=\rho/\rho_\infty$. The numerator in Eq. (57) provides the correct long time behavior. An expansion of the denominator can be performed and the unknowns b_1, b_2, and ρ_∞ obtained from the known coefficients $a_{\alpha1}$, $a_{\alpha2}$, and $a_{\alpha3}$ to provide the correct short time behavior.

We can also write an interpolation formula for the total surface coverage

$$\frac{\partial\theta}{\partial t}=\frac{\Sigma^2(1-x)^3}{1+c_1x+c_2x^2+c_3x^3} , \tag{58}$$

where $\theta=\rho_\alpha+\Sigma^2\rho_\beta$ (recall that the densities are in dimensionless form). The leading term of Eq. (58) is not unity but rather Σ^2, reflecting the area of β particles that fill the surface initially in the limit of infinitely fast spreading. The three coefficients can be solved in terms of the coefficients of $\partial\theta/\partial t$, which have the form $a_{\alpha i}+(\Sigma^2-1)a_{\beta i}$, and the condition that as $t\to\infty(x\to1)$, $\partial\rho/\partial t$ and $\partial\theta/\partial t$ approach zero in a similar fashion, as shown in Ref. [15]:

$$1+b_1+b_2=\frac{1+c_1+c_2+c_3}{\Sigma^2} . \tag{59}$$

Equations (57) and (58) can be integrated numerically in time to yield $\rho(t)$ and $\theta(t)$ and from them the partial densities $\rho_\alpha(t)=(\Sigma^2-1)^{-1}[\Sigma^2\rho(t)-\theta(t)]$ and $\rho_\beta(t)=(\Sigma^2-1)^{-1}[\theta(t)-\rho(t)]$.

Figure 3 compares results of the above interpolation formula to results from simulation. Notice that the agreement with simulation is good and the interpolation method improves significantly the approximation provided solely by the low-density expansion to third order. Figure 4 shows the total density, the partial densities, and the coverage at saturation predicted by the direct interpolation formula along with those calculated via simulation. Considering the difficulty in predicting saturation values from low-density series expansions, the agreement is quite satisfactory except when Σ approaches unity,

where the predicted curve does not reproduce the nonanalytic behavior (see Ref. [15]). In the finite spreading case, the direct interpolation scheme is inefficient due to our having calculated the low-density expansion only to second order.

B. Effective area method

To treat the general case of a finite rate of spreading (the effective area interpolation scheme is equally applicable to the case of infinitely fast spreading, but will be introduced here in the context of a finite rate of spreading, that is, the explicit dependence on the variable ζ will be noted), we propose to map the kinetics of adsorption of the RSA with spreading model onto the solution for standard RSA by defining an effective particle area $a_{\rm eff}(\rho,\zeta)$, from which one can write an effective surface coverage $\theta_{\rm eff}(\rho,\zeta)=\rho a_{\rm eff}(\rho,\zeta)$. The idea is that $a_{\rm eff}(\rho,\zeta)$ changes with ρ in such a way that at all times or at all densities $\Phi_\alpha(\rho,\zeta)$ from Eq. (34) equals $\Phi^{(0)}(\theta_{\rm eff}(\rho,\zeta))$, where

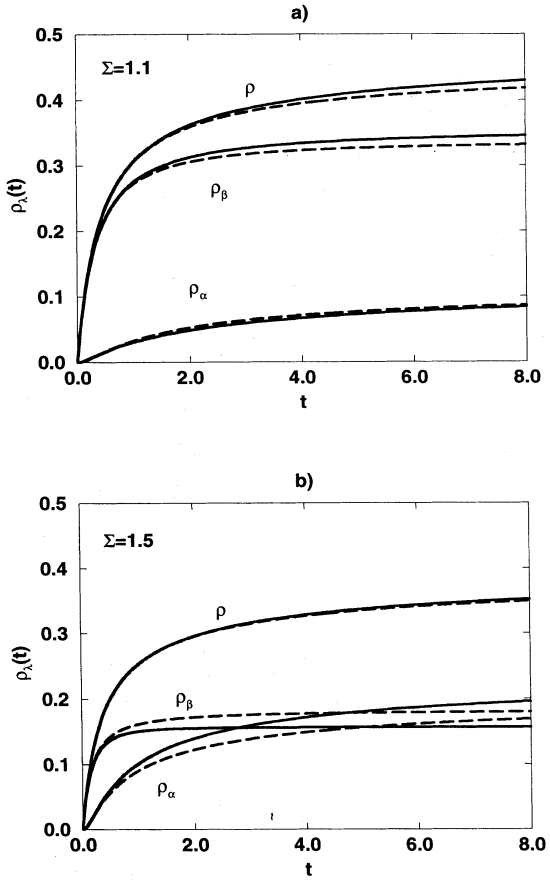

FIG. 3. Direct interpolation calculation (dashed line) of the reduced total and partial densities as functions of reduced time for instantaneous spreading ($K_s\to+\infty$) with (a) $\Sigma=1.1$ and (b) $\Sigma=1.5$. Also shown are simulation results (solid line).

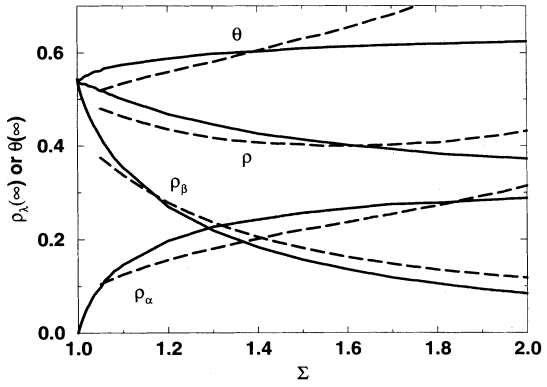

FIG. 4. Direct (dotted line) interpolation calculation of the total density, the coverage, and the partial densities at saturation for instantaneous spreading as functions of spreading magnitude. Also shown are simulation results (solid line).

$\Phi^{(0)}(\theta)$is the available surface function for standard RSA. Such a procedure is suggested by the experimental results of Ramsden [6] in which the data for the adsorption of the protein transferring are analyzed in terms of kinetic equations for the standard RSA of disks, but the average particle area (an adjustable parameter) changes with $k_a c$, i.e., with bulk protein concentration (see also Ref. [5]). Since we are looking for an approximate interpolation formula, we use for $\Phi^{(0)}(\theta)$ one of its very accurate approximants, e.g., [16]

$$\Phi^{(0)}(\theta)=\frac{(1-y)^3}{1+d_1y+d_2y^2+d_3y^3}\ , \tag{60}$$

where $y=\theta/\theta_\infty^{(0)}$ and $\theta_\infty^{(0)}$ equals the known saturation coverage for circular disks (i.e., 0.547 . . .) and d_1, d_2, and d_3 are determined from the fist three known coefficients of the density expansion for the standard RSA of disks.

Knowing the low coverage expansion of $\Phi^{(0)}(\theta)$ and the low density of $\Phi_\alpha(\rho,\zeta)$ up to second order and replacing θ by $\rho a_{\rm eff}(\rho,\zeta)$, one can obtain the low-density expansion of $a_{\rm eff}(\rho,\zeta)$ for fixed ζ up to first order. It is convenient to express $a_{\rm eff}(\rho,\zeta)$ as a simple Padé ratio of polynomials

$$a_{\rm eff}(\rho,\zeta)=\frac{a_{\rm eff0}(\zeta)}{1+a_{\rm eff1}(\zeta)\rho}\ , \tag{61}$$

where the coefficients $a_{\rm eff0}$ and $a_{\rm eff1}$ are expressed in terms of the coefficients $a_{\alpha1}(\zeta)$ and $a_{\alpha2}(\zeta)$ of Eqs. (41) and (55) and the known first- and second-order coefficients $a_1^{(0)},a_2^{(0)}$ of the coverage expansion of $\Phi^{(0)}(\theta)$ as

$$a_{\rm eff0}(\zeta)=\frac{a_{\alpha1}(\zeta)}{a_1^{(0)}}\ , \tag{62}$$

$$a_{\rm eff1}(\zeta)=\frac{a_2^{(0)}a_{\alpha1}(\zeta)}{a_1^{(0)2}}-\frac{a_{\alpha2}(\zeta)}{a_{\alpha1}(\zeta)}\ . \tag{63}$$

The saturation coverage ρ_∞ may be determined via an

iterative solution of the relation

$$\rho_\infty = \frac{\theta_\infty^{(0)}}{a_{\rm eff}(\rho_\infty)} = \frac{\theta_\infty^{(0)}}{a_{\rm eff0}(\zeta_\infty) - \theta_\infty^{(0)} a_{\rm eff1}(\zeta_\infty)} , \tag{64}$$

where $\zeta_\infty = K_s \rho_\infty$. Integration of Eq. (60) gives the time evolution of the total number density. Note that the above procedure ensures that the asymptotic approach towards saturation goes properly as $\rho_\infty - \rho(t) \sim t^{1/2}$.

A comparison of the above interpolation formula with simulation and experimental data is shown in Figs. 5–8 and is discussed below. In order to go beyond the description of the evolution of the total density and derive approximations for the partial densities, one may treat the kinetics of the total coverage in the same spirit as done above for the total density. The time evolution of the total surface coverage may be obtained by first noting that

$$\frac{\partial \theta}{\partial t} = \frac{\partial \theta}{\partial \rho} \frac{\partial \rho}{\partial t} = \bar{a}(\rho,\zeta) \frac{\partial \rho}{\partial t} = \bar{a}(\rho) \Phi^0(a_{\rm eff}(\rho,\zeta)\rho) , \tag{65}$$

where all partial derivatives are performed by taking K_s and ζ constant and where $\bar{a}(\rho,\zeta)$ is the average area of particles that land on the surface when the surface density is ρ; therefore, unlike the mapping variable $a_{\rm eff}(\rho,\zeta)$, it has a quantitative physical interpretation. To accelerate the convergence of the series in ρ, we use Padé approximants for $\bar{a}(\rho,\zeta)$, more specifically,

$$\bar{a}(\rho,\zeta) = \frac{\bar{a}_0(\zeta)}{1 + \bar{a}_1(\zeta)\rho + \bar{a}_2(\zeta)\rho^2} , \tag{66}$$

where $\bar{a}_0(\zeta)$ and $\bar{a}_1(\zeta)$ are obtained from the low-density expansion and $\bar{a}_2(\zeta)$ is adjusted to satisfy the constraint $\bar{a}(\zeta_\infty = \rho_\infty K_s) = 1$, which ensures that $\partial\theta/\partial t$ and $\partial\rho/\partial t$ are asymptotically equal when $t \to +\infty$ [15]:

$$\bar{a}_0(\zeta) = a_{\alpha 0}(\zeta) + (\Sigma^2 - 1) a_{\beta 0}(\zeta) , \tag{67}$$

$$\bar{a}_1(\zeta) = a_{\alpha 1}(\zeta) - \frac{a_{\alpha 1}(\zeta) + (\Sigma^2 - 1) a_{\beta 1}(\zeta)}{a_{\alpha 0}(\zeta) + (\Sigma^2 - 1) a_{\beta 0}(\zeta)} , \tag{68}$$

$$\bar{a}_2(\zeta) = \frac{[a_{\rm eff0}(\zeta) - \theta_\infty^{(0)} a_{\rm eff1}(\zeta)]^2 [\bar{a}_0(\zeta) - 1]}{(\theta_\infty^{(0)})^2} - \frac{[a_{\rm eff0}(\zeta) - \theta_\infty^{(0)} a_{\rm eff1}(\zeta)]}{\theta_\infty^{(0)}} , \tag{69}$$

where $\theta_\infty^{(0)} = 0.547\cdots$. Clearly, other forms of Eq. (66), i.e., different Padé polynomial ratios, could be used as well. Any choice, though, must go to unity at long times and, when multiplied by $\partial\rho/\partial t$, reproduce the low-density expansion of $\partial\theta/\partial t$.

The time evolution of the total and partial densities predicted by the effective area interpolation scheme and calculated by simulation are shown for the case of instantaneous spreading (Fig. 5) and for finite spreading rates (Figs. 6 and 7). We observe excellent agreement between the effective area method's predicted total number density (which also happens to be the experimentally accessible variable) with simulation. For the partial densities, the predictions are less accurate. However, of particular interest is the ability of the theory to capture the nonmonotonic behavior of the α particles at a large (but finite) value of K_s. For smaller K_s, this maxima occurs at a higher density and so cannot be recovered by this low-density expansion technique.

Figure 8 shows the total density, the coverage, and the partial densities predicted by the effective area method at saturation as a function of spreading magnitude along with those calculated via simulation, for several spreading rates. Except in the limit of $\Sigma \to 1$, we observe reasonably good agreement for the total density and the partial densities at $K_s = 10$ and $K_s = \infty$. The partial densities have qualitatively correct trends, but assume incorrect values in the limit of $\Sigma \to 1$. Despite requiring coefficients only to second order, the effective area interpolation scheme is, in the case of instantaneous spreading, at least as accurate as the direct interpolation scheme. For $K_s = 1$, the partial densities are in error for the reasons cited above. Figure 9 shows the effective area

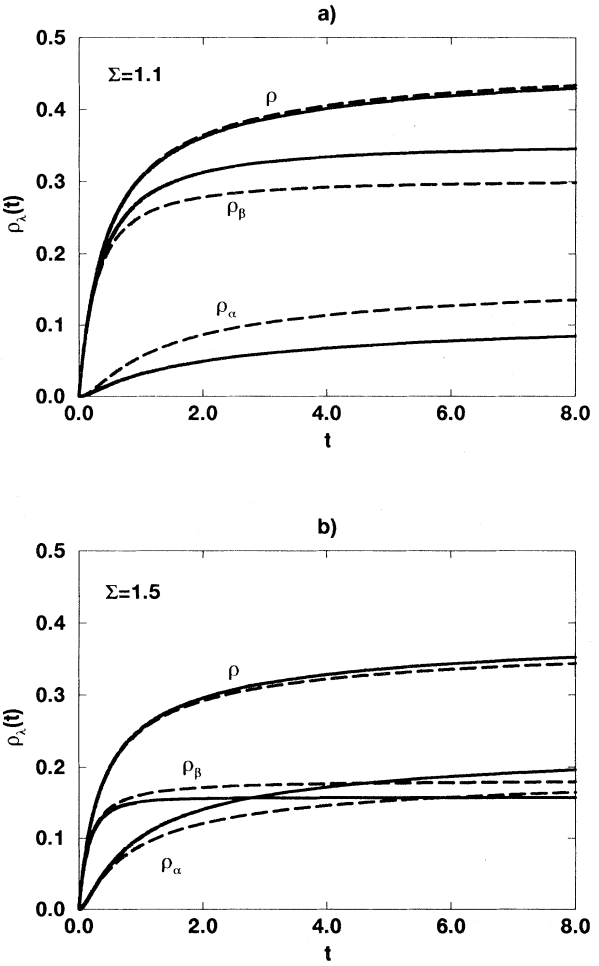

FIG. 5. Effective area interpolation calculation (dashed line) of the reduced total and partial densities as functions of reduced time for $K_s = \infty$ and (a) $\Sigma = 1.1$ and (b) $\Sigma = 1.5$. Also shown are simulation results (solid line).

$a_{\text{eff}}(\rho,\zeta=K_s\rho)$ and the average area of particles landing on the surface at density ρ, $\bar{a}(\rho,\zeta)$, as a function of density for different values of K_s. The nonmonotonic behavior of $\bar{a}$ for finite spreading is a consequence of the process that fixes two limits: at short times, adsorbing particles have not had sufficient time to spread, and at long times, the surface is too crowded to allow for any spreading. In both limits, $\bar{a}(\rho=0,\zeta)=1$. Note that discontinuities exist for both a_{eff} and $\bar{a}$ upon going form a finite to infinite spreading rate; a_{eff} and $\bar{a}$ approach unity as $\rho\to 0$ for finite K_s and $(\Sigma+1)^2/4$ and Σ^2, respectively, for infinite K_s.

V. COMPARISON WITH EXPERIMENT

Recently, optical methods [6] have been developed that allow for the accurate measurement of protein adsorption kinetics and are thus able to discriminate between adsorption models. In Fig. 10 we compare the rates of adsorption versus surface density predicted by the effective area interpolation method with the experimental results for the protein transferrin [5] for two different bulk concentrations. The experimental comparison requires four parameters: the rate of deposition k_a, the particle area per mass a/m, and the model parameters Σ and K_s. We have not performed a best fit but rather have chosen parameters that are consistent with their known approximate values and with comparisons made in Ref. [15]. Table I summarizes the parameter choice. Note that the same parameters are used for both concentrations.

We also present in Fig. 10 the prediction of a Langmuir-like model, which assumes a trivial surface blockage for both adsorption and conformational change [23,24]. It is characterized by the kinetic equations

$$\frac{\partial\rho_\alpha}{\partial t}=(1-K_s\rho_\alpha)(1-\rho_\alpha-\Sigma^2\rho_\beta)\ , \tag{70}$$

$$\frac{\partial\rho_\beta}{\partial t}=K_s\rho_\alpha(1-\rho_\alpha-\Sigma^2\rho_\beta)\ . \tag{71}$$

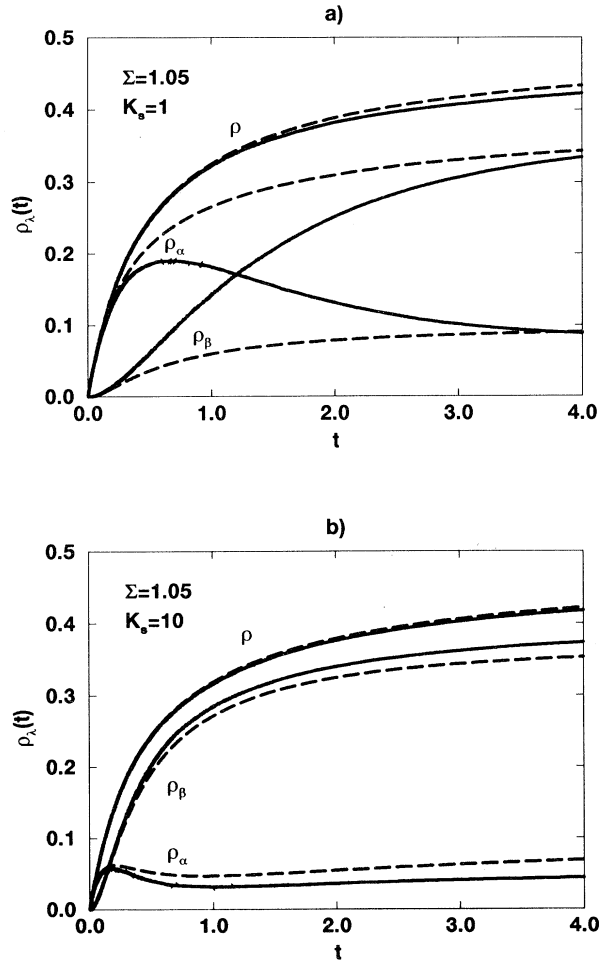

FIG. 6. Effective area interpolation calculation (dashed line) of the reduced total and partial densities as functions of reduced time for $\Sigma=1.05$ and (a) $K_s=1$ and (b) $K_s=10$. Also shown are simulation results (solid line).

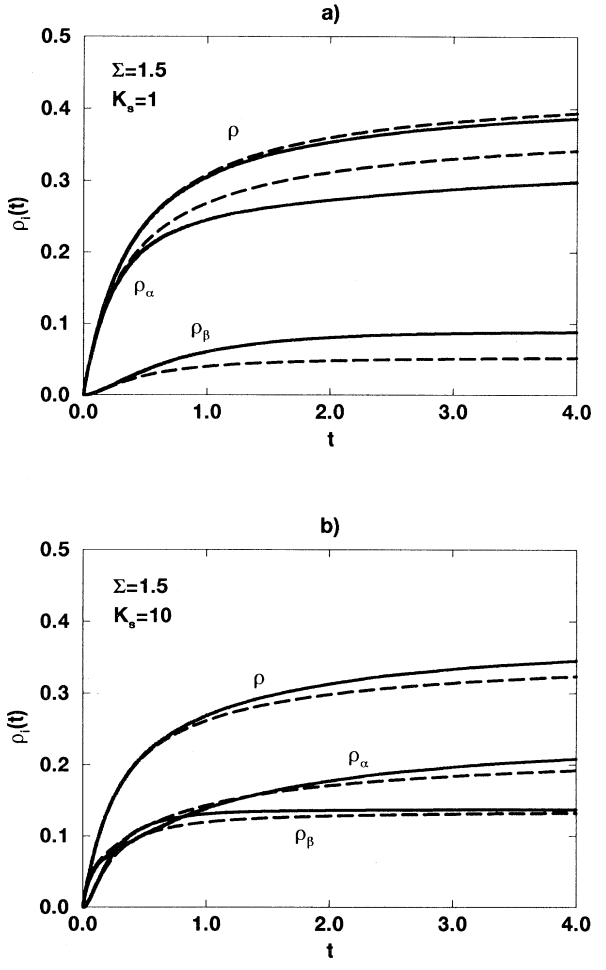

FIG. 7. Effective area interpolation calculation (dashed line) of the reduced total and partial densities as functions of reduced time for $\Sigma=1.5$ and (a) $K_s=1$ and (b) $K_s=10$. Also shown are simulation results (solid line).

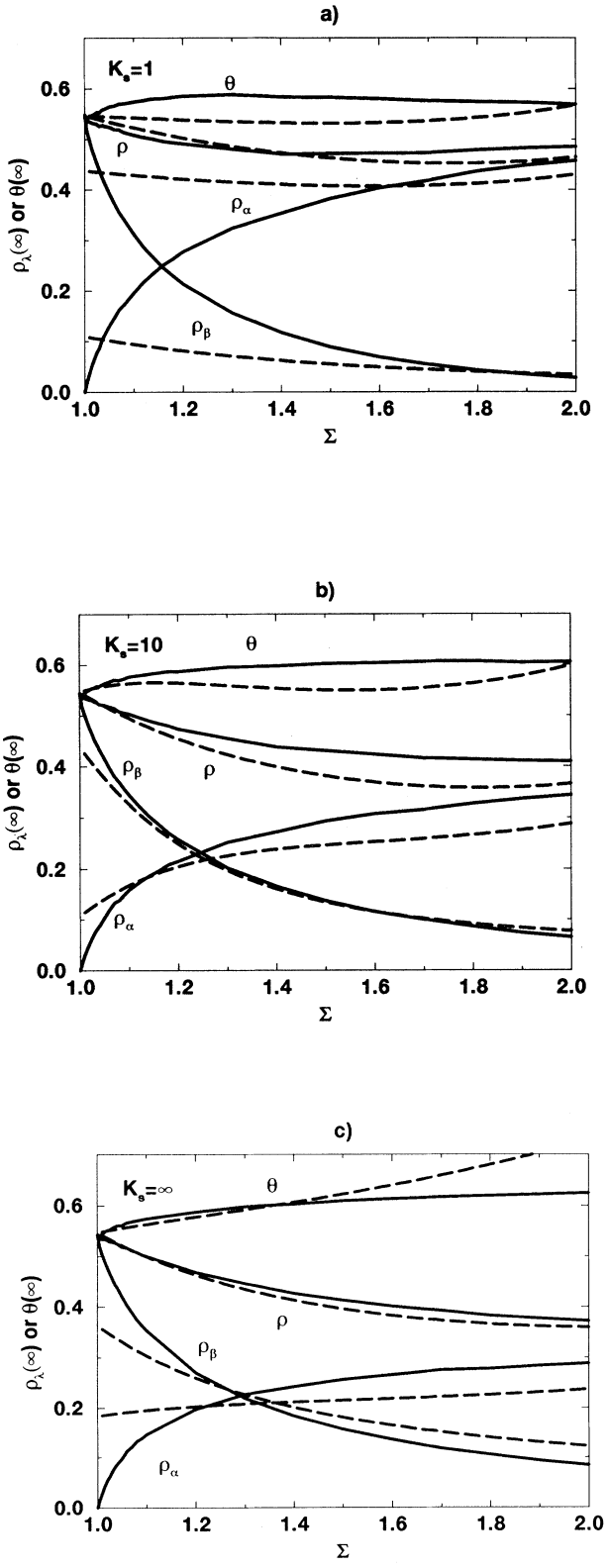

FIG. 8. Effective area interpolation calculation (dashed line) of the total density, the coverage, and the partial densities at saturation as functions of spreading magnitude for finite spreading rate (a) $K_s=1$, (b) $K_s=10$, and (c) $K_s=\infty$. Also shown are simulation results (solid line).

This approach essentially replaces both Φ_α and $\Psi_{\alpha\beta}$ in Eqs. (30) and (31) by $(1-\rho_\alpha-\Sigma^2\rho_\beta)$. One could also introduce a desorption rate in the Langmuir-like model as discussed in Ref. [24], but for the present experimental situation it would be inappropriate since desorption was shown to be negligible. The result is a rate of adsorption that exhibits negative curvature, a feature not at all in accord with the experimental data. In contrast, the approach presented here clearly accounts for the adsorption kinetics with positive curvature observed experimentally (Fig. 10).

VI. CONCLUSION

We present here a theoretical analysis of the kinetics of the random sequential adsorption of spreading hard disks using a low-density expansion formalism. When the spreading rate is infinite, a straightforward expansion

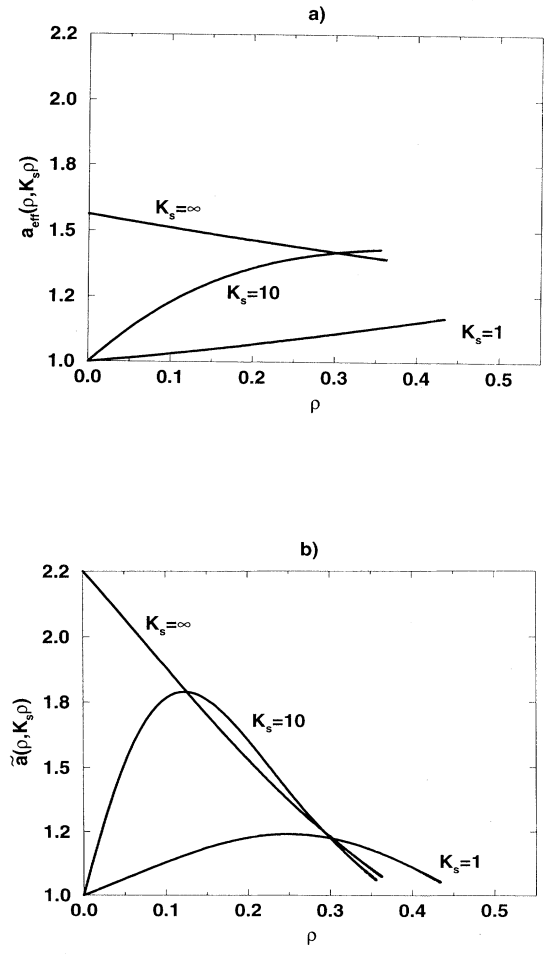

FIG. 9. (a) $a_{\text{eff}}(\rho,\zeta=\rho K_s)$ and (b) $\tilde{a}(\rho,\zeta=\rho K_s)$ as functions of spreading magnitude for different values of K_s. Note that discontinuities exist for both $a_{\text{eff}}(\rho,\rho K_s)$ and $\tilde{a}(\rho,\rho K_s)$ at $\rho=0$ upon going from a finite to an infinite spreading rate.

TABLE I. Parameters used in the experimental comparison of Fig. 10. Parameters were chosen to provide a good fit between the effective area interpolation model and experiment and to be in accord with previous estimates. The same parameters were used to compare the Langmuir model of Eqs. (70) and (71), except that a/m values of 1.5 and 1.7 cm^2/ng were required to fit the Langmuir model at $c=9.4$ and 20 $\mu g/cm^3$, respectively.

Parameter	Chosen value	Estimated value and source
k_a	1.4×10^{-4} cm/s	1.09×10^{-4} cm/s as calculated by the relation of Lévèque [25]
a/m	1.4 cm^2/ng	1.4–1.5 cm^2/ng as estimated via experiment [5]
Σ	1.6	1.6 as given by the best fit in a previous experimental comparison [15]
K_s	20	between 0.3 and 30 as estimated via experiment [5]

may be performed, as was done for standard RSA [11]. When the spreading rate is finite, a renormalization is required and the coefficients can be obtained as the solutions to first-order differential equations. Interpolation formulas may be used to connect the low-density regime to the known asymptotic behavior to predict the total and partial densities accurately at all times. This represents a good approximate solution to a complicated nonequilibrium statistical mechanical problem involving surface exclusion and time-dependent surface structural relaxation. It also provides tractable analytical formulas to interpret experimental data on protein adsorption when desorption from the surface is negligible.

ACKNOWLEDGMENTS

We are grateful to Jeremy Ramsden for providing experimental data. The authors wish to thank the Centre Européen de Calcul Atomique et Moléculaire, the Centre National de la Recherche Scientifique, and the National Science Foundation for financial support of this work. P.R.V.T. wishes to thank the Chateaubriand program for financial support. We are particularly grateful to Professor Giovanni Ciccotti for helpful support and discussions during the preparation of this manuscript. The Laboratoire Physique Théorique des Liquides is Unité de Recherche No. 765 associée au Centre National de la Recherche Scientifique.

APPENDIX

The form of the coefficients of the density expansion of Φ_λ are given as

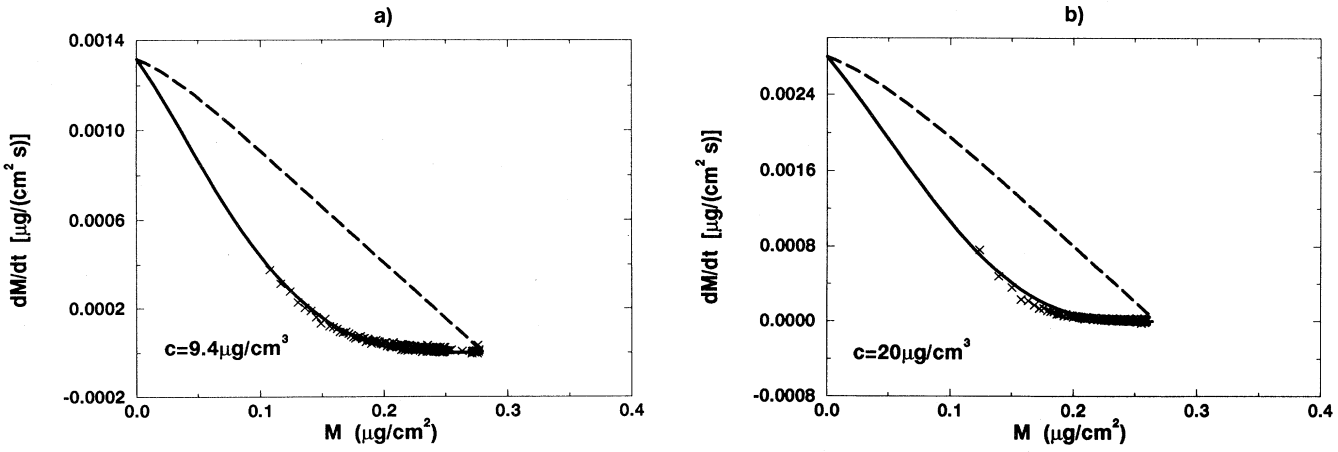

FIG. 10. Rate of adsorption as a function of surface density predicted by the effective area interpolation model (solid line), the Langmuir-with-spreading model (dashed line) [25], and experimental results for the protein transferrin (data points) [5]. The theoretical results have been converted to experimental units via the reported area per adsorbed transferrin [5] and by matching the rate of deposition at low coverage. Experimental bulk protein concentrations are 9.4 and 20 $\mu g/cm^3$. Parameters used are discussed in Table II.

$$a_{\lambda 1}=\int d2\, f_{12}^{\lambda\beta}\ , \tag{A1}$$

$$a_{\lambda 2}=\tfrac{1}{2}\int d2\,d3(f_{12}^{\lambda\alpha}-f_{12}^{\lambda\beta})(f_{13}^{\alpha\beta}-f_{13}^{\beta\beta})+\tfrac{1}{2}\int d2\,d3\, f_{12}^{\lambda\beta}f_{13}^{\lambda\beta}(1+f_{23}^{\beta\beta})+\tfrac{1}{2}\int d2\,d3\, f_{12}^{\lambda\alpha}f_{13}^{\lambda\beta}(f_{23}^{\alpha\beta}-f_{23}^{\beta\beta})\ , \tag{A2}$$

$$\begin{aligned}a_{\lambda 3}=&\tfrac{1}{6}\int d2\,d3\,d4(f_{12}^{\lambda\alpha}-f_{12}^{\lambda\beta})[(f_{13}^{\alpha\beta}-f_{13}^{\beta\beta})(f_{14}^{\alpha\alpha}-4f_{14}^{\alpha\beta}+f_{14}^{\beta\beta})+(f_{13}^{\alpha\beta}f_{14}^{\alpha\beta}-f_{13}^{\beta\beta}f_{14}^{\beta\beta})(1+f_{34}^{\beta\beta})\\&+(f_{13}^{\alpha\alpha}f_{14}^{\alpha\beta}-f_{13}^{\alpha\beta}f_{14}^{\beta\beta})(f_{34}^{\alpha\beta}-f_{34}^{\beta\beta})]\\&+\tfrac{1}{6}\int d2\,d3\,d4\, f_{12}^{\lambda\alpha}f_{13}^{\lambda\alpha}[(f_{14}^{\alpha\beta}-f_{14}^{\beta\beta})(f_{23}^{\alpha\alpha}-f_{23}^{\alpha\beta})+f_{34}^{\alpha\beta}(1+f_{23}^{\alpha\alpha})(f_{24}^{\alpha\beta}-f_{24}^{\beta\beta})-f_{34}^{\beta\beta}(1+f_{23}^{\alpha\beta})(f_{24}^{\alpha\beta}-f_{24}^{\beta\beta})]\\&+\int d2\,d3\,d4\, f_{12}^{\lambda\beta}f_{13}^{\lambda\beta}(1+f_{23}^{\beta\beta})\{\tfrac{1}{6}f_{34}^{\alpha\beta}(f_{24}^{\alpha\beta}-f_{24}^{\beta\beta})-\tfrac{1}{2}(f_{14}^{\alpha\beta}-f_{14}^{\beta\beta})+\tfrac{1}{3}f_{34}^{\beta\beta}f_{24}^{\beta\beta}\}\\&+\int d2\,d3\,d4\, f_{12}^{\lambda\alpha}f_{13}^{\lambda\beta}[\tfrac{1}{6}f_{24}^{\alpha\alpha}(1+f_{23}^{\alpha\beta})(f_{34}^{\alpha\beta}-f_{34}^{\beta\beta})+\tfrac{1}{3}f_{24}^{\alpha\beta}f_{34}^{\beta\beta}(1+f_{23}^{\alpha\beta})+\tfrac{1}{6}f_{34}^{\beta\beta}(f_{24}^{\alpha\beta}-f_{24}^{\beta\beta})\\&\qquad-\tfrac{1}{6}f_{24}^{\alpha\beta}(1+f_{23}^{\beta\beta})(f_{34}^{\alpha\beta}-f_{34}^{\beta\beta})-\tfrac{1}{3}f_{24}^{\beta\beta}f_{34}^{\beta\beta}(1+f_{23}^{\beta\beta})+\tfrac{1}{2}(f_{14}^{\alpha\beta}-f_{14}^{\beta\beta})(1+f_{23}^{\beta\beta})]\\&+\tfrac{1}{6}\int d2\,d3\,d4\, f_{12}^{\lambda\alpha}f_{13}^{\lambda\alpha}f_{14}^{\lambda\beta}(1+f_{23}^{\alpha\alpha})(1+f_{24}^{\alpha\beta})(1+f_{34}^{\alpha\beta})[f_{24}^{\beta\beta}f_{34}^{\beta\beta}+\tfrac{1}{2}f_{23}^{\alpha\beta}(f_{34}^{\beta\beta}+f_{24}^{\beta\beta})+f_{24}^{\beta\beta}f_{34}^{\beta\beta}f_{23}^{\alpha\beta}]\\&+\tfrac{1}{6}\int d2\,d3\,d4\, f_{12}^{\lambda\alpha}f_{13}^{\lambda\beta}f_{14}^{\lambda\beta}(1+f_{23}^{\alpha\beta})(1+f_{24}^{\alpha\beta})(1+f_{34}^{\beta\beta})[-\tfrac{3}{2}(f_{23}^{\beta\beta}+f_{24}^{\beta\beta})-f_{23}^{\beta\beta}f_{24}^{\beta\beta}]\\&+\tfrac{1}{6}\int d2\,d3\,d4\, f_{12}^{\lambda\beta}f_{13}^{\lambda\beta}f_{14}^{\lambda\beta}(1+f_{23}^{\beta\beta})(1+f_{24}^{\beta\beta})(1+f_{34}^{\beta\beta})\ .\end{aligned} \tag{A3}$$

All the integrals in Eqs. (A1) and (A2) can be determined analytically or numerically via a one-dimensional integral. These are given as

$$a_{\alpha 1}=-(1+\Sigma)^2\ ; \tag{A4}$$

$$a_{\beta 1}=-4\Sigma^2\ ; \tag{A5}$$

$$\begin{aligned}a_{\alpha 2}=&8\left[\frac{(1+\Sigma)^2}{4}-\Sigma^2\right]+\frac{4}{\pi}(1+\Sigma)^2\left[\left[\Sigma^2-\frac{(1+\Sigma)^2}{4}\right]\sin^{-1}\left[\frac{\Sigma}{(1+\Sigma)}\right]+\frac{3}{4}\Sigma\sqrt{1+2\Sigma}\right]\\&-\frac{2}{\pi}\Sigma(1+2\Sigma)^{3/2}+\frac{16}{\pi}\int_{(1+\Sigma)/2}^{\Sigma}dr\, r\left[\cos^{-1}(x)-x\sqrt{1-x^2}+\frac{(1+\Sigma)^2}{4}[\cos^{-1}(y)-y\sqrt{1-y^2}]\right]\ ,\end{aligned} \tag{A6}$$

with

$$x=\frac{r^2-(1+\Sigma)^2/4+1}{2r},\quad y=\frac{r^2+(1+\Sigma)^2/4-1}{r(1+\Sigma)}\ ; \tag{A7}$$

$$a_{\beta 2}=8\left[\frac{(1+\Sigma)^2}{4}-\Sigma^2\right]^2+\frac{6\sqrt{3}}{\pi}\Sigma^2+\frac{16}{\pi}\int_{(1+\Sigma)/2}^{\Sigma}dr\, r\left[\frac{(1+\Sigma)^2}{4}[\cos^{-1}(x)-x\sqrt{1-x^2}]+\Sigma^2[\cos^{-1}(y)-y\sqrt{1-y^2}]\right]\ , \tag{A8}$$

with

$$x=\frac{r^2+(1+\Sigma)^2/4-\Sigma^2}{r(1+\Sigma)},\quad y=\frac{r^2-(1+\Sigma)^2/4+\Sigma^2}{2r\Sigma}\ . \tag{A9}$$

Only a few of integrals appearing in Eq. (A3) may be determined in this way. Instead, we evaluate this coefficient as a function of Σ via a Monte Carlo integration scheme that samples points in space randomly. Values of these coefficients as functions of Σ are given in Table II.

TABLE II. Coefficients of the density expansion of Φ_λ given in Eq. (6) for various values of the spreading magnitude Σ.

Σ	$a_{\alpha 1}$	$a_{\alpha 2}$	$a_{\alpha 3}$	$a_{\beta 1}$	$a_{\beta 2}$	$a_{\beta 3}$
1.0	−4.000	3.308	1.407	0	0	0
1.1	−4.410	4.080	1.793	−4.840	5.324	1.739
1.2	−4.840	5.101	2.348	−5.760	8.231	1.964
1.3	−5.290	6.421	2.463	−6.760	12.244	0.479
1.4	−5.760	8.089	2.375	−7.840	17.595	−2.737
1.5	−6.250	10.161	2.231	−9.000	24.548	−9.953
1.6	−6.760	12.695	1.887	−10.240	33.363	−22.507

[1] J. D. Andrade, *Surface and Interfacial Aspects of Biomolecular Polymers,* edited by J. D. Andrade (Plenum, New York, 1985), Vol. 2.
[2] W. Norde, Adv. Colloid Interface Sci. **25**, 267 (1986).
[3] W. Norde, F. MacRitchie, G. Nowicka, and J. Lyklema, J. Colloid Interface Sci. **112**, 447 (1986).
[4] P. Schaaf, P. Déjardin, A. Johner, and A. Schmitt, Langmuir **8**, 514 (1992).
[5] J. J. Ramsden, Phys. Rev. Lett. **71**, 295 (1993); J. Stat. Phys. **73**, 853 (1993).
[6] J. J. Ramsden, Q. Rev. Biophys. **27**, 41 (1993).
[7] J. Feder and I. Giaever, J. Colloid Interface Sci. **78**, 144 (1980).
[8] G. Y. Onoda and E. G. Liniger, Phys. Rev. A **33**, 715 (1986).
[9] Z. Adamczyk, B. Siwek, and M. Zambala, J. Colloid Interface Sci. **151**, 351 (1992), and references therein.
[10] P. Schaaf and J. Talbot, Phys. Rev. Lett. **62**, 175 (1989).
[11] G. Tarjus, P. Schaaf, and J. Talbot, J. Stat. Phys. **63**, 167 (1991).
[12] J. W. Evans, Rev. Mod. Phys. **65**, 1281 (1993).
[13] Z. Adamczyk, B. Siweck, M. Zembala, and P. Belouschek, Adv. Colloid Surf. **48**, 151 (1994).
[14] D. Boyer, J. Talbot, G. Tarjus, P. R. Van Tassel, and P. Viot, Phys. Rev. E **49**, 5525 (1994).
[15] P. R. Van Tassel, P. Viot, G. Tarjus, and J. Talbot, J. Chem. Phys. **101**, 7064 (1994).
[16] P. Schaaf and J. Talbot, J. Chem. Phys. **91**, 4401 (1989).
[17] R. Dickman, J. S. Wang, and I. Jensen, J. Chem. Phys. **94**, 8252 (1994).
[18] S. M. Ricci, J. Talbot, G. Tarjus, and P. Viot, J. Chem. Phys. **101**, 9164 (1994).
[19] G. Tarjus, P. Schaaf, and J. Talbot, J. Chem. Phys. **93**, 8352 (1990).
[20] A. P., Thompson and E. D. Glandt, Phys. Rev. A **46**, 4639 (1992).
[21] G. Tarjus, P. Viot, H. Choi, and J. Talbot, Phys. Rev. E **49**, 3239 (1994).
[22] J. W. Evans, Phys. Rev. Lett. **62**, 2641 (1989).
[23] I. Lundström, Phys. Scr. **T4**, 5 (1983).
[24] J. D. Andrade and V. Hlady, Adv. Polym. Sci. **79**, 1 (1986), and references therein.
[25] M. A. Lévèque, Ann. Mines **13**, 201 (1928); **13**, 305 (1928); **13**, 381 (1928).